A THESIS FOR THE DEGREE OF MASTER OF SCIENCE

Analysis of Canopy Photosynthesis Using 3D Paprika Model and Ray-Tracing Simulation

3 차원 광선 추적 시뮬레이션을 이용한 파프리카 군락의 광합성 분석

BY

JEEHOON KIM

FEBRUARY, 2015

MAJOR IN HORTICULTURAL SCIENCE AND BIOTECHNOLOGY
DEPARTMENT OF PLANT SCIENCE
GRADUATE SCHOOL
COLLEGE OF AGRICULTURE AND LIFE SCIENCES
SEOUL NATIONAL UNIVERSITY

Analysis of Canopy Photosynthesis Using 3D Paprika Model and Ray-Tracing Simulation

UNDER THE DIRECTION OF DR. JUNG EEK SON
SUBMITTED TO THE FACULTY OF THE GRADUATE SCHOOL OF SEOUL NATIONAL UNIVERSITY

BY
JEEHOON KIM

DEPARTMENT OF PLANT SCIENCE
COLLEGE OF AGRICULTURE AND LIFE SCIENCES
SEOUL NATIONAL UNIVERSITY

FEBRUARY, 2015

APPROVED AS A QULIFIED THSIS OF JEEHOON KIM
FOR THE DEGREE OF MASTER OF SCIENCE
BY THE COMMITTEE MEMBERS

CHAIRMAN:

_____
CHANG HOO CHUN, Ph.D

VICE-CHAIRMAN:

_____
JUNG EEK SON, Ph.D

MEMBER:

_____
KI SUN KIM, Ph.D

Analysis of Canopy Photosynthesis Using 3D Paprika Model and Ray-Tracing Simulation

Jeehoon Kim

Dept. of Plant Science, Graduate School of Seoul National University

ABSTRACT

Canopy photosynthesis has typically been estimated using mathematical models that have the following assumptions: the light interception inside the canopy exponentially decays in a vertical distribution, and the photosynthetic capacity is proportional to the light interception as a result of acclimation. However, in actual situations, light interception in the canopy is quite different depending on several environmental factors such as the location, microclimate, leaf area index, and canopy architecture, and it is important to apply these variances in an analysis. The objectives of the current study are to estimate the canopy photosynthesis of paprika (*Capsicum annuum* L.) with an analysis of the intercepted irradiation of the canopy using a 3D ray-tracing simulation and by applying a photosynthetic capacity in each layer. By inputting the structural data of an actual plant, the 3D architecture of paprika could be developed using graphic software. With a 3D virtual plant, simulations were conducted using ray-tracing software. Depending on the sunlight properties, the vertical distributions of intercepted irradiance within the plant were dynamically altered, and their patterns were also changed according to the time of day. The light curve and A/C_i curve of each layer were measured, and the parameters of the photosynthetic capacity used in the Farquhar, von Caemmerer and Berry (FvCB) model were determined at each layer. The photosynthetic capacity within the plant was significantly different among the vertical positions. With the intercepted irradiation data and photosynthetic parameters of each layer, the values of an entire plant's photosynthesis rate were

estimated by integrating the calculated photosynthetic rate at each layer. The estimated photosynthesis rate of an entire plant showed good agreement with the measured plant using a closed chamber for validation. By expanding this approach to canopy conditions, it is possible to analyse the canopy's photosynthesis as a key factor in a cultivation system.

Additional key words: 3D model, ray tracing simulation, canopy photosynthesis, light interception, light use efficiency, Paprika, photosynthetic parameters

Student Number: 2013-21105

CONTENTS

LIST OF TABLES

LIST OF FIGURES

INTRODUCTION

Canopy photosynthesis is the key factor for estimating crop growth and establishing the strategy of CO_2 fertilization inside a greenhouse. Because crop yield is closely related to the seasonal integral of the total canopy photosynthesis, it can be used as base data to predict the crop production in a greenhouse. Additionally, by estimating the attenuation of CO_2 concentration with time, supply rates of CO_2 fertilization would be determined in a cultivation system. In general, canopy photosynthesis is primarily determined by the light regime inside the greenhouse, and several variances must be considered. Scaling up from the leaf to the canopy, the vertical pattern of the intercepted irradiation can be affected by the vertical structure of the whole plant and additional shading effects would occur from neighbouring plants in the canopy. Other variances such as the direction of the sunlight, the ratio of the diffuse light, the greenhouse structure, the plant growth stage, and the plant density also affect the intercepted irradiation inside the canopy. Therefore, in estimating the canopy's photosynthesis, it is important to investigate the light interception of the plant surface caused by these variances.

However, it is difficult to measure the actual light interception of the plant surface because of technical limitations. Therefore, previous research has estimated the canopy's photosynthesis through a modelling approach that depends on various mathematical equations. Among the various approaches, the single leaf models, such as the FvCB model (Farquhar *et al.*, 1980), represent the leaf level physiological mechanism, and the whole canopy models, including the sunlit-shaded model (de Pury & Farquhar, 1997), are the most well-known models for the photosynthesis model (Zhu *et al.*, 2012). Although these models are useful, they have rarely been used in horticultural species (Gonzalez & Baille, 2000). Primary assumptions are that the absorbed photosynthetic active radiation is proportional to the photosynthetic capacity through the canopy to maximize the entire canopy's photosynthesis (Field 1983; Hirose & Werger, 1987; Leaning, 1995; de Pury & Farquhar, 1997). Additionally, to simplify

the calculation procedures, models have assumed that the vertical distribution of light interception has a negative exponential pattern from the top to the bottom of the canopy (Monsi & Saeki, 1953). As mentioned in several previous papers, the high level of spatial and temporal heterogeneity of the light interception is not considered in these models, for example, the effect of a sun fleck on the lower part of the canopy, diffuse radiation which penetrates deep into the canopy (Terashima & Hikosaka, 1995; de Pury & Farquhar, 1997; Zhu *et al.*, 2012), and the plant architecture affected by the leaf shape and angle in the light interception (Elias *et al.*, 1989; Ellsworth & Reich, 1993; Kim *et al.*, 2010).

Furthermore, differences in quantum yield within the plant should be provided in the calculation of canopy photosynthesis. Assessing the vertical variation in leaf photosynthesis among different positions is required to investigate how carbon and nutrient resources are partitioned within the canopy (Field, 1983). Similar to the vertical pattern of light interception, many models fixed the pattern of the photosynthetic capacity using a negative-exponential function and assumed that the spatial distribution of the leaf nitrogen contents as a photosynthetic capacity had an identical pattern of light interception as a result of the acclimation from the light environment at each position (Sims & Pearcy 1992; J.R. Evans & Poorter, 2001; Boonman *et al.*, 2007).

For analysis of the canopy photosynthesis rate, it is essential to develop a detailed analysis tool and method that considers various environmental factors. From this perspective, the construction of a 3D graphic plant is necessary to reflect the precise physical properties of the plant structure, and a ray-tracing technique is a reasonable solution to incorporate optical properties such as the reflectance and transmittance of a leaf and other structures in the light interception data. Thus, the objectives of the current study are to analyse accurate light interception data in various conditions using a 3D ray-tracing method, determine the vertical

distributions of photosynthetic parameters using experimental data, and calculate the photosynthesis rate of each layer as well as the canopy photosynthesis.

LITERATED REVIEW

Canopy photosynthesis model

Canopy photosynthesis models provided theoretical frameworks for analysis of the scaling of physiological processes (de Pury and Farquhar, 1997). Elements of the canopy photosynthesis depended on the biochemical capacity such as amounts of Rubisco and RuBP, temperature, intercellular CO_2 concentration and absorbed irradiation. The FvCB model, the well-known model of photosynthesis, covered these detailed physiological and ecological perspectives.

The sunlit-shaded model using the FvCB model has been the best performer over a wide range of different time scales and had major advantage on its scalability to incorporate leaf level physiological properties to canopy level (Zhu *et al.*, 2012). The photosynthetic capacity of canopy (V_c) consisted of two parts: sunlit and shaded parts. In the same way, absorbed irradiance within the canopy (I_c) was separately calculated by integrating the absorbed PAR of sunlit (I_{csun}) and shaded (I_{csh}) fractions in this model. Summarized equations are as following.

$$A_c = A_{csun}, f\left(V_{csun,}\, I_{csun}\right) + A_{csh,}\, f\left(V_{csh,}\, I_{csh}\right) - R_c \quad (1)$$

$$V_c = V_{csun} + V_{csh} \quad (2)$$

$$I_c = I_{csun} + I_{csh} \quad (3)$$

where A_c is canopy photosynthesis rate, A_{csun} and A_{csh} are photosynthesis rates of sunlit fraction and shaded fractions, respectively.

Although it is the most powerful model of the existing canopy models, a major limitation was to predict the ‘average’ light intensities for both sunlit and shaded fractions within the canopy. The heterogeneity of light environments inside the canopy was not considered such as

a sun fleck or shading effect by other leaves or plants (Norman, 1980;. de Pury and Farquhar, 1997; Zhu *et al.*, 2012). Furthermore, calculation of the absorbed irradiation highly relies on mathematical equations and the accuracy of photosynthesis model is required against the complexity and the increase in the number of additional calculations required (Norman, 1980).

Correlations of light acclimation and nitrogen distribution

Profiles of leaf properties have been explained by the assumption that the leaves adapt to their light environment such that nitrogen resources in plant may be distributed to maximize daily canopy photosynthesis (Field, 1983; Hirose and Werger, 1987). Optimal distribution of nitrogen inside the entire plant could be maintained when any re-allocation of nitrogen would decrease the photosynthesis rate of the entire plant (de Pury and Farquhar, 1997). Additional hypothesis explained the acclimation of leaves that nitrogen is distributed in proportion to the distribution absorbed irradiance, usually averaged irradiance over a week (Zhu *et al.*, 2012).

In terms of the photosynthetic partitioning, plants remobilize carbon and nitrogen from senescencing leaves at the lowest layer of a canopy to re-use for the growth of new leaves at the top of the canopy. This process usually happens when the photosynthetic CO_2 uptake of bottom leaves is less than its respiratory cost (Hikosaka, 2005; Anten and During, 2011). The leaf N profile changed during crop development and was responsive to N availability. At high N supply, the leaf N profile was constant during crop development, in contrast at low N supply, the N distributions fluctuated between more uniform and steep patterns. These changes were associated with reduced leaf area expansion and increasing N remobilization from bottom leaves (Dreccer *et al.*, 2000). Physiological interaction between N distribution and other environment factors should be engaged in further research and must be incorporated to canopy photosynthesis model for the estimation of canopy photosynthesis dynamically.

MATERIALS AND METHODS

Cultivation conditions

This experiment was conducted in a Venlo-type glasshouse located at the experimental farm of the Seoul National University in Suwon, Korea (37.3° N, 127° E, 30 m.a.s.l.). Paprika plants (*Capsicum annuum* L.) were transplanted after 3 months (20 July – 15 Oct. 2014) in rock wool cubes with a plant density of 3 plants/m^2 and the distance between rows was 80 cm. Air conditioners were installed in each wall of the glasshouse to maintain a temperature between 25 and 35°C inside the greenhouse during the summer season and the relative humidity was controlled to be within a range of 60–80% using fogging systems. Nutrient solutions were irrigated 4 times a day at 10:00, 12:00, 14:00 and 16:00. To prevent a deficit of N related to the biosynthesis of chlorophylls, the total N concentration in the nutrient solution was NO_3-N 110 mg/l. The other concentrations of macro-elements in the nutrient solution included P 50 mg/l, K 140 mg/l, Ca 160 mg/l, Mg 45 mg/l, and S 60 mg/l. The EC and pH ranges of the nutrient solutions were 2.6–3.0 dS/m and 5.5–6.5, respectively. The plants were pruned to form two main stems, which were vertically trellised to a 'V' canopy system (Jovicich *et al.*, 2004).

Leaf photosynthesis and leaf nitrogen measurements

Five samples with a similar height, node number, and tip node length representing specific growth stages were chosen from a total of 90 plants. Eight layers were divided within each sample plant to investigate the vertical pattern of the leaf photosynthetic capacity. Each layer consisted of four leaves except for the first layer, which had two leaves, and the sample layer number was determined to be 1 on the leaves of the first node and 15 on the leaves of the 15th node.

The leaf photosynthesis of each layer was measured with a portable photosynthesis system (LI-6400, LI-COR, USA). A closed chamber on the photosynthesis system was set at 25°C for

the leaf temperature and 60–70% for the relative humidity to obtain the photosynthetic parameters on the standard temperature condition. Additionally, a red 8:blue 2 light quality of an LED light source similar to the sun spectrum was used inside the closed chamber. By using the auto program of the light curve and an A/C_i curve that measures 20 points for each program, measurements of net photosynthesis were made at 1) a saturating photosynthetic photon flux density (PPFD) (I = 1000 μmol/$m^{2/}$s) with a varying external CO_2 partial pressure (p_a = 0–120 Pa) and 2) a saturating external CO_2 partial pressure (p_a = 100 Pa) with a varying I (50–1000 μmol/m^2/s). The calculated values of the internal CO_2 partial pressure (C_i) were provided by the LI-COR system inside the device.

After the photosynthesis measurement, each sample leaf was collected to determine the leaf nitrogen allocation at different positions within the plant. An average value of the leaf nitrogen content per layer was investigated after the Kjeldahl digestion of the leaves, which were oven-dried at 80°C for 5 days and then grounded.

Entire-plant photosynthesis measurements

To measure the daily CO_2 consumption of an entire plant, a closed chamber (1 m x 1 m x 2 m) was designed and constructed using transparent polycarbonate. To control environmental factors such as CO_2, temperature, and humidity, additional devices were installed inside the chamber as shown in Fig. 1; this is referred to as an open chamber system (Garcia, 1990). The CO_2 concentration inside the chamber was set to range between 80 and 200 Pa to measure the photosynthesis rate of the entire plant while maintaining a CO_2 level above the saturation points. An additional supply of CO_2 gas was implemented when the CO_2 concentration in the chamber was approximately 80 Pa. The difference between the internal and external CO_2 concentrations was detected using a CO_2 analyser (LI-820, LI-COR, USA). The seepage of CO_2 in the chamber was maintained at ± 2.5 Pa (data are not provided). Irradiance inside the chamber was measured

using an irradiation sensor (BF5, Delta-T Devices, UK) and the diffuse ratio was also determined. To maintain the temperature and CO_2 concentration inside the chamber, two radiators circulating cool water were placed along each sidewall. A fan was passed through the radiators and blown towards the chamber wall to maintain equal ventilation. The temperature inside the chamber was maintained at 25°C by circulating cooled water controlled by a condenser (DH-003A, Daeho-condenser, Korea). The CO_2 concentration, irradiance, and temperature inside the chamber were stored in a data logger every 10 seconds. To control the increased humidity from the respiration and transpiration of the plant, silica gel was used in the air circulation process. A plant was selected from among five samples and was placed in the chamber from 9:00 to 18:00. Whenever the CO_2 concentration reached approximately 100 Pa, additional CO_2 was supplied to retain a saturated CO_2 condition (Fig 2).

Construction of the 3D virtual plant

Before sealing the chamber for measuring the entire plant's photosynthesis, a sample plant free from disorders was chosen to design the 3D virtual plant. The structure of the sample plant was measured using a ruler and protractor to transpose the real structure of the plant to a 3D graphic. The architect parameters consisted of three major parts (leaf, petiole, and stem) and the detailed measurements included the following: 1) leaf area and leaf angle; 2) petiole length and petiole angle; and 3) stem length, stem diameter, and stem angle. The area of each leaf within the sample plant was measured using a leaf area meter (LI-3100, LI-COR, USA).

To design a 3D virtual plant, a 3D construction tool was developed using graphic software (Houdini FX, FX, Canada), as shown in Fig. 3. Using an L-system formalism, which is useful in the construction of a plant's growth pattern, the plant structure could be built up from the bottom to the top in the tree window (right-bottom window) by applying structure values for each part of the plant. For the validation procedure, the actual plant inside the closed chamber

was virtualized as a 3D graphic plant that referred to the measured values of the plant structure and the digitized data using a 3D digitizer (Sense, 3D systems, Inc., USA). The virtual plant consisted of two primary stems having 15 nodes each. The calculation of the leaf area (LA) is determined using the length (L) and width (W). The leaf area equation is embedded inside the graphic tool, LA= 0.6034 LW + 0.0732 (R^2 = 0.994, p value < 0.001) (Tai *et al*., 2009). The leaves with an accurate leaf area were simultaneously shown on the graphic window when the users input the values of L and W (left window). The leaf angles were also applied by inputting the angles (x, y, z) of the directions, and the angles of the petiole were corrected using the droopiness parameter in the parameter window (right-upper window).

Simulation of the intercepted irradiation

Redesigning the 3D plant was accomplished using 3D CAD software (SOLIDWORKS, Dassault Systemes, FRANCE), and light interception analysis was simulated using ray-tracing software (OPTISWORKS, OPTIS Inc., FRANCE). 3D detectors were placed on the surface of the leaves in the canopy plants to investigate the intercepted irradiance in specific conditions and values of light intensity were obtained on the 3D leaf surface. With the simulation software it was possible to input microclimate parameters: sun directions (coordinates, date, time, zenith, north direction), and sunlight properties (ratio of direct light and diffuse light); and material parameters: optical properties of the leaf, chamber, and glasshouse structure. Optical properties (transmittance and reflectance) were measured using an integrating sphere (IC2, StellarNet Inc., CANADA) with a spectrometer (BLUE-Wave, StellarNet Inc., CANADA) and a light source (SL1 Tungsten Halogen, StellarNet Inc., CANADA) and entered in the preferences section for the leaves in the simulation program. In the leaf optical measurements, the optical properties of the leaves have little differences in the vertical position within the plant; the average reflectance was 30% regardless of the wavelengths, with a small peak at 560 nm and the

average transmittance was only 15% at 550 nm. Ray-tracing simulations were conducted with 10 giga rays and the number of max impacts was set to be 10 for all conditions. Identifying the applicability for expanding to a canopy situation, plant arrays of 1 x 1, 3 x 3, and 5 x 5 were set to investigate the different patterns of intercepted radiation. Detectors were placed on the surface of a single plant located in the centre of the canopy. Four cases were simulated at 9:00, 12:00, 15:00 and 18:00 and the intercepted irradiance was analysed for each layer.

Calculation of the photosynthetic parameter

The prediction of the leaf photosynthesis rate was based on the FvCB model (Eq. 4).

$$A_l = \min\begin{Bmatrix} A_v, f(V_{lm}, c_i, T_l) \\ A_j, f(I, f, J_m, c_i, T_l) \end{Bmatrix} - R_l, f(T_l) \quad (4)$$

where A_l is the rate of the leaf's net assimilation, and A_v and A_j indicate the rates of the leaf gross assimilation limited by ribulose biphosphate-carboxylase-oxygenase (Rubisco) activity and ribulose biphosphate (RuBP) regeneration, respectively. Divided into two limited parameters, A_l is determined by the minimum value of the two rates. Each rate can be expressed as various leaf characteristics (the maximum photosynthetic Rubisco capacity, V_{lm}, and the maximum rate of electron transport, J_m). All of the temperature conditions in the current experiment were fixed at 25 °C to neglect the effect of temperature on the parameters and, therefore, on the temperature-related functions in the model.

The maximum photosynthesis rate (A_{max}) was calculated from the light curve at each layer by using a non-rectangular hyperbolic function. The photosynthetic Rubisco capacity (V_l) was also obtained from the A/C_i curve by using a non-linear regression. Assuming that the CO_2 fixation rate is limited only by Rubisco activity in a low CO_2 condition, and V_l value of each layer was estimated from the A/C_i curve of each layer within the range $C_i < 30$ Pa (Eq. 5).

Similarly, the potential rate of the electron transport (J_m) values was determined from the A/C_i curve at a range above 40 Pa for C_i (Eqs. 6 and 7).

$$V_l = A_v \frac{(c_i + K')}{(c_i - \Gamma_*)} \quad (5)$$

$$J = 4A_j \frac{(c_i + 2\Gamma_*)}{(c_i - \Gamma_*)} \quad (6)$$

$$J_m = J \frac{(I_{le} - \theta_l J)}{(I_{le} - J)} \quad (7)$$

where I_{le} is the photosynthetically active radiation (PAR) effectively absorbed by PSII, and J is the rate of electron transport. Detailed model equations and constants are shown in Tables 1 and 2.

Validation of an entire plant's photosynthesis rate

With an average value of intercepted irradiation from the simulation and photosynthetic parameters from the measurements at each layer, the leaf photosynthesis rate was calculated for each layer. To apply the actual light intensity from the logged data to an estimate, the average values of light intensity and the diffuse ratio were determined using a simple moving average method with a 15-minute time scale. By integrating the photosynthesis rate at each layer, the photosynthesis rate of the entire plant was calculated using Eq. 8.

$$A_c = \sum_{1}^{L=8} \{A_l(2L-1) - R_l(2L-1)\} \quad (8)$$

For example, at 504.8 μmol/m^2/s of light intensity above the plant and a diffuse ratio of 43%, at 13:00 on Oct. 15, 2014, the entire plant's photosynthesis could be calculated as A_c = (0.80 + 0.78 + 0.77 + 0.92 + 1.15 + 1.23 + 1.59 + 1.77) - (0.18 + 0.29 + 0.50 + 0.61 + 0.63 + 0.69 + 0.72 + 0.78) = 4.61 μmol/m^2/s. The values of A_l(15) and A_l(1) were 1.77 and 0.80 μmol/m^2/s and the values of R_l(15) and R_l(1) calculated using Eq. A7 in Table 2 were 0.78 and 0.18

μmol/m^2/s, respectively. According to this method, the estimated data were calculated every half hour and these data of the entire plant's photosynthesis rate were compared with actual data from 9:00 to 18:00 on Oct. 15, 2014, for validation. From an actual measurement of the CO_2 concentration in a sealed chamber, the reduction of the CO_2 concentration was converted to a photosynthesis rate assuming that the slope of the CO_2 concentration is the same as the photosynthesis rate.

RESULTS

Distribution of the maximum photosynthesis rate and leaf nitrogen content within the entire plant

The maximum photosynthesis rate, A_{max}, at each layer was measured to be within 1000 μmol/m^2/s of the light intensity and 100 Pa of the CO_2 saturation condition as shown in Fig. 4. The mean values of A_{max} decreased from the top (layer 15) to the bottom (layer 1), from 37.04 to 12.41 μmol/m^2/s, respectively. The standard variations of A_{max} were somewhat higher in the upper part than the bottom, indicating that the range of A_{max} appeared broader in the younger leaves compared to the older leaves at the bottom. Unlike the exponential patterns generally assumed in many photosynthesis models, the distribution of A_{max} for an individual plant showed a linear pattern on all of the five sample plants.

In the case of nitrogen distribution, the total nitrogen content in each leaf increased with an increase in the leaf layer number. Although the standard deviation in the middle layer was greater, the total nitrogen content in the uppermost layer was more than double that in the bottom layer, similar to A_{max}, and it was apparent that most of the nitrogen was allocated to the upper layer, which retained higher light use efficiency (Fig. 4). Decreasing patterns of A_{max} and N_{tot} were very similar in the vertical distribution, indicating that the nitrogen content is strongly correlated with the photosynthetic capacity. Converting a leaf nitrogen content on a dry mass basis (mg/g) to a leaf nitrogen concentration on a leaf area basis (g/m^2), the spatial distribution of the nitrogen content on a leaf area basis was not significantly meaningful.

Distribution of photosynthetic parameters, V_{lo} and J_{mo}, within an entire plant

Comparing the light curves and A/C_i curves at each layer, the photosynthetic capacity in a certain position varied considerably among the layers, resulting in different light use efficiencies. Changes in V_{lo} and J_{mo} were identified by the leaf position using the measured

value of A_l for each layer at 25°C (Table 3). By increasing the leaf layer number, both the average values of V_{lo} and J_{mo} decreased from 88.62 and 175.42 (layer 15) to 20.31 and 50.83 μmol/m^2/s (layer 1), respectively. Despite significant variations, both average values of the parameters showed linear patterns in the vertical distribution rather than exponential patterns within the plant, similar to A_{max} and N_{tot}. Average values of photosynthetic parameters were selected to use in the calculation of the photosynthesis rate at each layer.

Validation of an entire plant's photosynthesis and expansion to the canopy situation

Half hour-photosynthetic rates of the sample plant were compared with estimated rates and showed good agreement with a coefficient of determination (R^2) of 0.85 (Fig. 5). The estimation values were slightly lower than actual values before 11:00 and after 13:00, whereas estimates were higher than actual values for only three points at midday. Daily variations in the photosynthesis rates were clearly shown in the estimated data.

For the canopy situation, the 3D simulated data explicitly shows the shading effect of the neighbouring plants, which mostly appeared in the middle and bottom layers (Fig. 6). From an overhead view the intercepted irradiance within the plant was primarily affected by the plant, which was oriented towards the sun. The total intercepted radiation of the centre plant surrounded by eight plants did not decrease significantly regardless of the number of neighbouring plants and the shade time determined by the height of the neighbouring plants. In estimating the intercepted irradiation at each layer, linear decay appeared at the top and middle layers, and the variations in the intercepted irradiation occurred as a result of the changes in sun direction (Fig. 7).

DISCUSSION

Canopy photosynthesis is such a complex mechanism that the correlation of various environmental factors engaged in the photosynthesis process should be considered. Furthermore, scaling up from leaf to canopy, the leaf properties related to the photosynthetic capacity within the canopy should be considered at different accumulated light environments. Therefore, it is necessary to clarify the relationship between light acclimation and nitrogen distribution, which is also heterogeneous within the canopy. Intercepted radiation is sensitively affected by leaf shape, leaf angle and plant position inside the canopy architecture (Ellsworth & Reich, 1993; Gonzalez & Baille, 2000; Sarlikioti *et al.*, 2011); therefore, precise measurement of intercepted radiation on the plant surface is not easy because of technical limitations.

Accordingly, a 3D model is necessary for an analysis of intercepted irradiation. Furthermore, to obtain the precise architecture for a plant in a 3D model, advanced technology for scanning the material is required to simulate the intercepted radiation on the plant surface, and the supporting hardware should be accompanied by an increased number of rays in the optical simulation. In actual canopy conditions, the heterogeneity of plant architecture still exists such that the compromise between precision and simplicity is inevitable in analysing canopy photosynthesis. A simplified analysis method with guarantee of its accuracy is strongly required to perceive dynamic changes of the canopy photosynthesis rate in real-time.

With regards to the photosynthetic capacity, the spatial distribution of nitrogen allocation provides another method for estimating canopy photosynthesis. Standard deviations of the nitrogen content exist primarily in the middle layers, indicating that the heterogeneity of the light environment in the canopy primarily occurred as a result of additional influences such as a sun fleck or shading effect by neighbouring plants. Although many researchers determined

the optimal distribution of nitrogen in nature to be a method for maximizing canopy photosynthesis (Hirose & Weger, 1991; Schieving *et al.*, 1992), the detailed mechanism of leaf acclimation to the light environment remains under investigation including the quantitative analyses of photosynthetic capacity (Ellsworth & Reich, 1993; Atsuhiro *et al.*, 2005; Iio *et al.*, 2005; Anten & During, 2010). The spatial distribution of nitrogen within the canopy is greatly simplified by models to calculate the canopy photosynthesis, and fixing the pattern of the photosynthetic parameters may cause errors in the precise estimation of canopy photosynthesis. In the current study, the leaf layer criteria of paprika were simplistically established because of the plant architecture pattern. However, additional criteria might be required for other species such as leafy vegetables that have a horizontal structure rather than a vertical structure.

In addition, other environmental factors such as the external CO_2 concentration, temperature, and leaf age also affect the leaf properties of photosynthesis (Field, 1983; Escudero & Mediavilla, 2003; Thornley, 2010). It was assumed in this research that the spatial distributions of the external CO_2 concentration and temperature are identical within the canopy. Paprika transplanted after 3 months were chosen in the current analysis because of the closed chamber's size limitations. In applying later growth stages, the conditions for the analysis should be modified because the intercepted radiation is changed by neighbouring plants whose heights are greater. Furthermore, leaf age functions should be incorporated into the FvCB model (Irving & Robinson, 2006) to estimate the photosynthesis of each leaf for different growth stages within the canopy.

In spite of several existing limitations in estimating the canopy's photosynthesis, the simulation method developed is quite suitable for precisely predicting the canopy's photosynthesis rate by applying microclimatic factors such as the location, date, time, diffuse ratio, and optical properties of the materials. From the simulated data, the sun fleck inside the canopy was found to change with time and the average light intensity of a certain layer depends

on the amount of direct sunlight. Furthermore, fractions of sunlit and shaded areas changed through time, with the result that the vertical distributions of intercepted radiation did not always follow the pattern of the Lambert-Beer's law that irradiation is exponentially decayed. An increase in the diffuse ratio of sunlight reduces light variations among the leaves at different locations in the canopy. The current simulation results identified that the pattern of intercepted irradiation within the entire plant was strongly determined by sun direction and its optical properties.

CONCLUSION

In the current study, an analysis method to determine the canopy photosynthesis was developed using graphic software based on 3D model and ray-tracing simulation. The advantages of this method are the availability of precise analysis of canopy photosynthesis considering various environmental factors and the expendability to greenhouse cultivation condition. By supplementing plant physiological aspects, the method could be a powerful tool to predict the mass production of horticultural crops in greenhouses.

Table 1. Equations of the FvCB model.

Equation	Description	Number
$A_l = \min\{A_v, A_j\} - R_l$	Rate of leaf net photosynthesis	(A1)
$A_v = V_l \frac{(c_i - \Gamma_*)}{(c_i + K')}$	Rubisco-limited photosynthesis	(A2)
$K' = K_c \left(1 + \frac{O}{K_o}\right)$	Effective Michaelis-Menten constant	(A3)
$A_j = J \frac{(c_i - \Gamma_*)}{4(c_i + 2\Gamma_*)}$	Electron-transport limited rate of photosynthesis	(A4)
$\theta_l J^2 - (I_{le} + J_m)J + I_{le}J_m = 0$	Irradiance dependence of electron transport	(A5)
$I_{le} = \frac{I_l(1-f)}{2}$	PAR effectively absorbed by PS Ⅱ	(A6)
$\frac{R_l}{V_l} = \frac{\Gamma - \Gamma_*}{\Gamma + K'}$	Ratio of leaf respiration to photosynthetic Rubisco capacity	(A7)

* Temperature condition = 25 °C, other temperature-related functions are omitted

Table 2. Photosynthetic parameters and constants of the FvCB model at 25 °C.

Symbol	Value	Unit	Description
K_c	40.4	Pa	Michaelis-Menten constant of Rubisco for CO_2
K_o	24.8×10^3	Pa	Michaelis-Menten constant of Rubisco for O_2
O	20.5×10^3	Pa	Oxygen partial pressure
R_{lo}	$0.0089V_{lo}$	μmol/m^2/s	Leaf dark respiration rate
Γ	4.4	Pa	CO_2 compensation point of photosynthesis
Γ_*	3.69	Pa	Γ in the absence of mitochondrial respiration
f	0.15	—	Spectral correction factor
θ_l	0.7	—	Curvature of leaf response of electron transport to irradiance

*Values of the photosynthetic parameters are given at 25 °C.

Table 3. Estimation of the photosynthetic parameters V_{lo} (= value of V_l at 25 °C) and J_{mo} (= value of J_m at 25 °C). n and R^2 means number of observations per layer and coefficient of determination by fitting non-rectangular hyperbolae functions, respectively.

Layer	V_{lo}	n	R^2	J_{mo}	n	R^2
15	88.62±8.20[z]	35	0.76	175.42±13.17	134	0.71
13	81.72±5.74	34	0.83	123.97±9.77	102	0.78
11	77.93±6.24	34	0.70	119.64±9.87	124	0.85
9	71.25±5.60	32	0.80	107.64±11.84	132	0.75
7	68.56±6.88	33	0.69	88.63±12.47	126	0.69
5	56.08±7.09	36	0.73	72.62±14.08	118	0.73
3	32.82±7.70	32	0.66	67.49±14.66	102	0.67
1	20.31±2.57	29	0.88	50.83±10.69	92	0.73

[z] Mean±SE

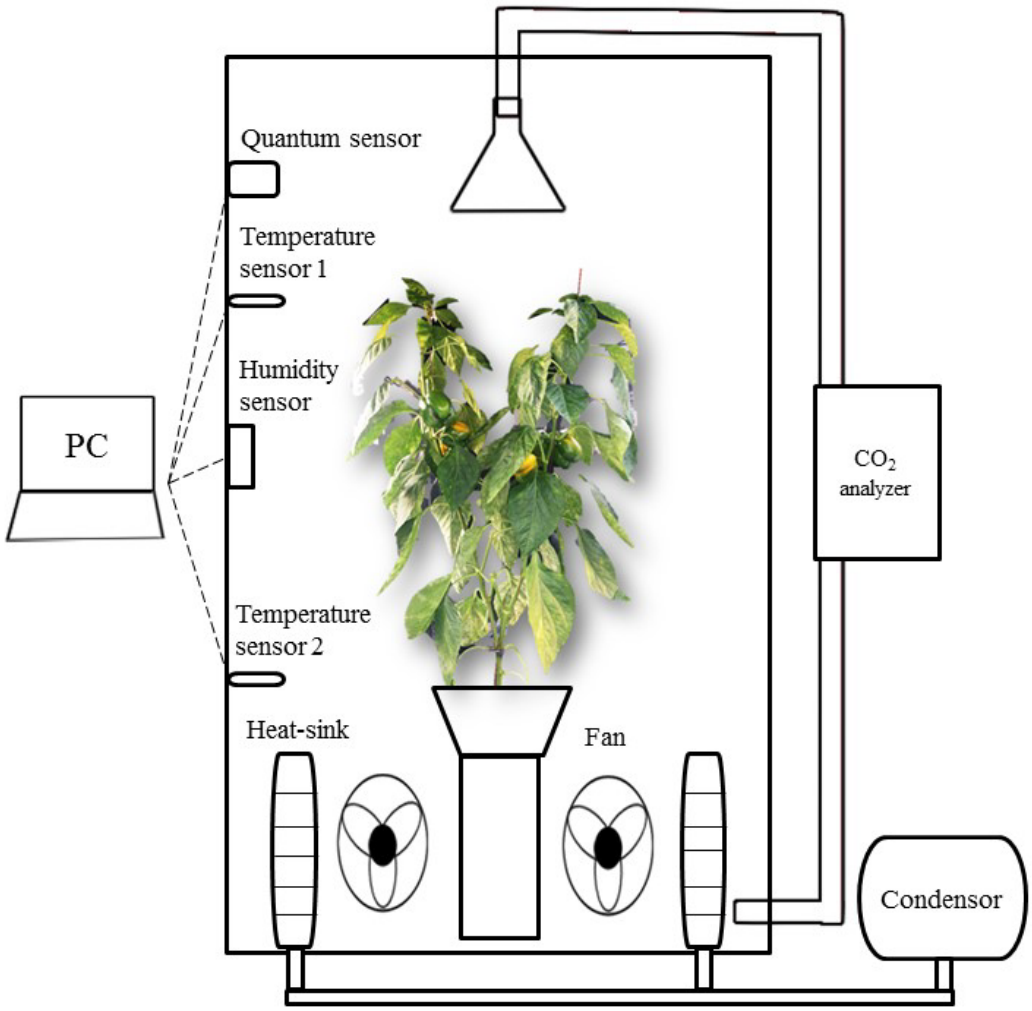

Fig. 1. A schematic diagram of a closed chamber for measuring CO_2 consumption.

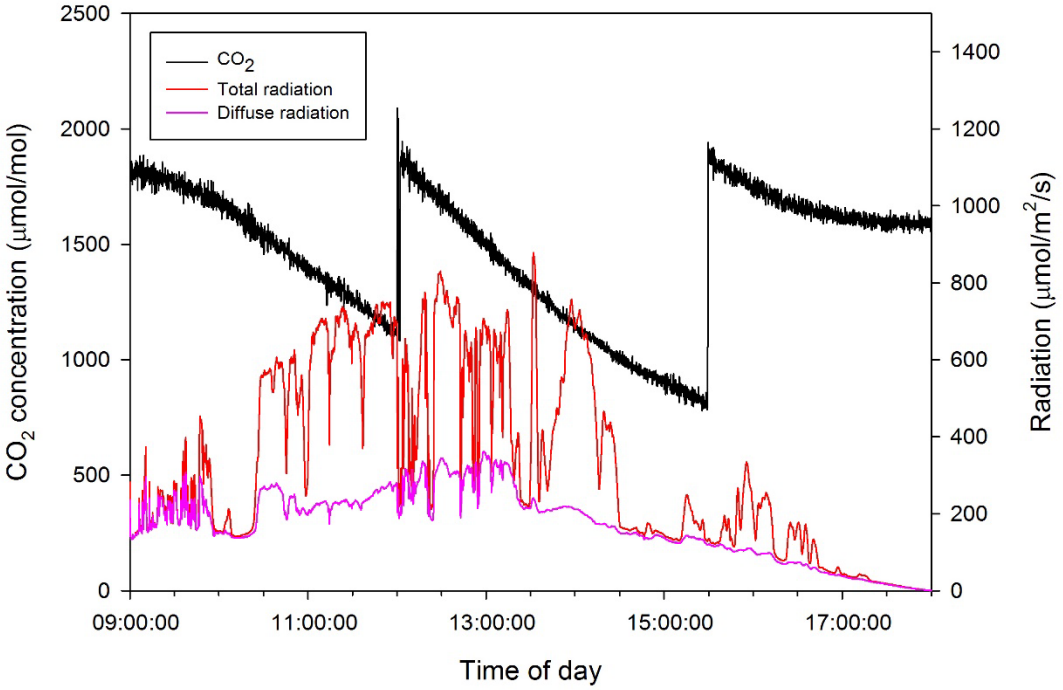

Fig. 2. Daily changes in CO_2 concentration in the closed chamber with light intensity above the plant on 15 Oct. 2014.

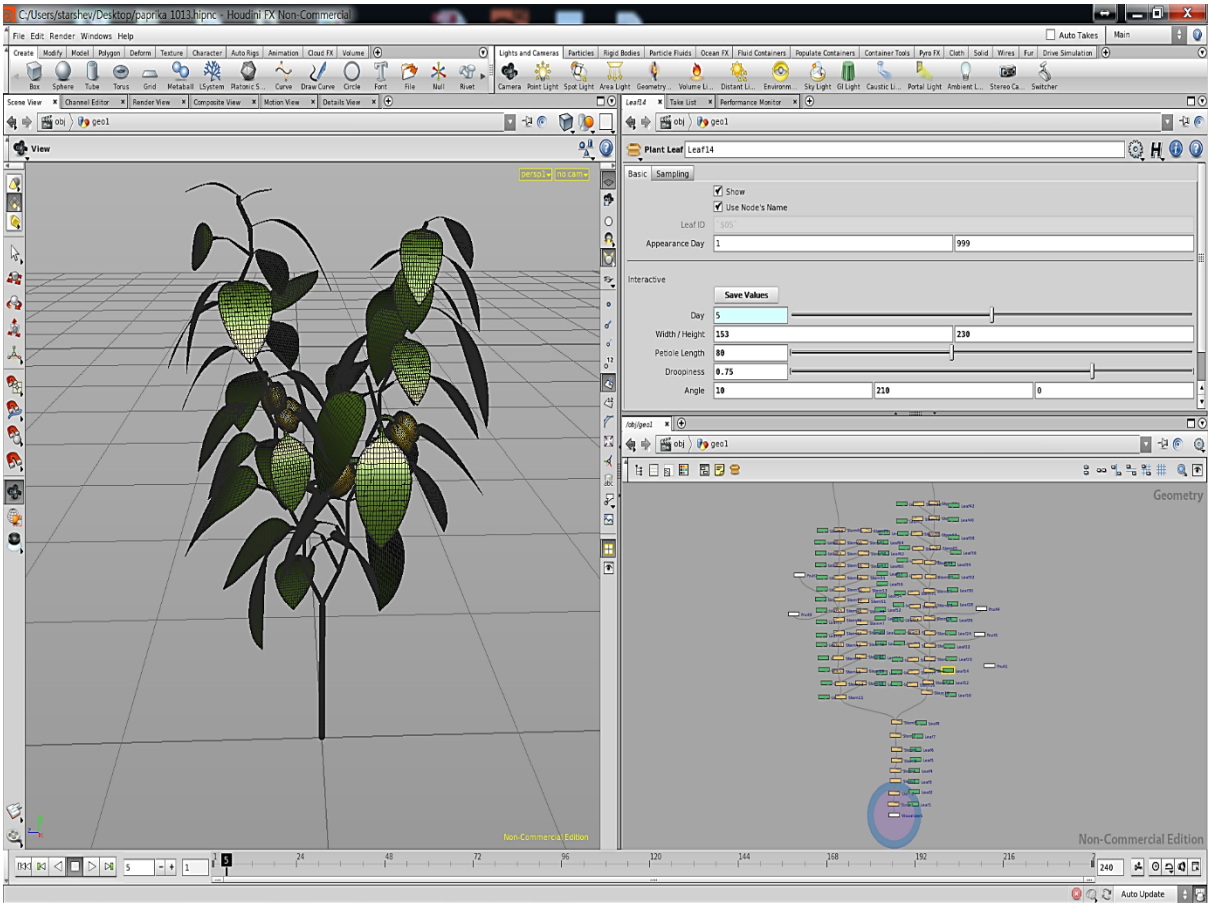

Fig. 3. A 3D virtual plant constructed in the L-system using the Houdini FX graphic software.

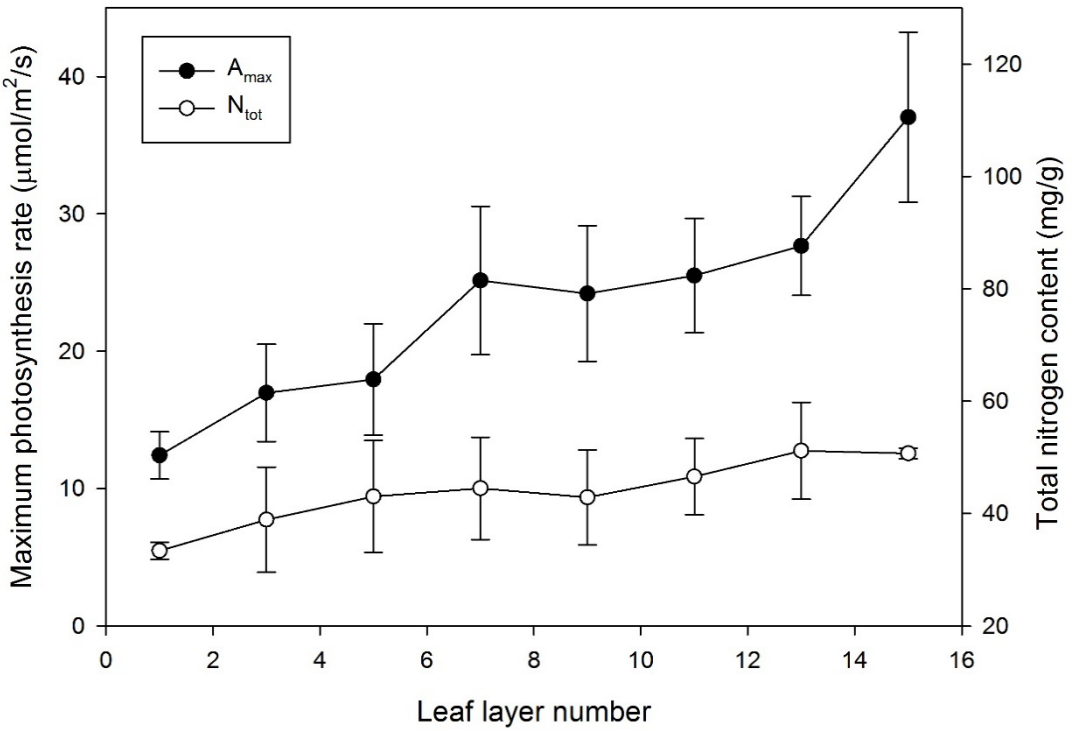

Fig. 4. Maximum photosynthesis rate (A_{max}) and total nitrogen content (N_{tot}) by leaf layer number. Vertical bars represent the Mean±SE (n = 5).

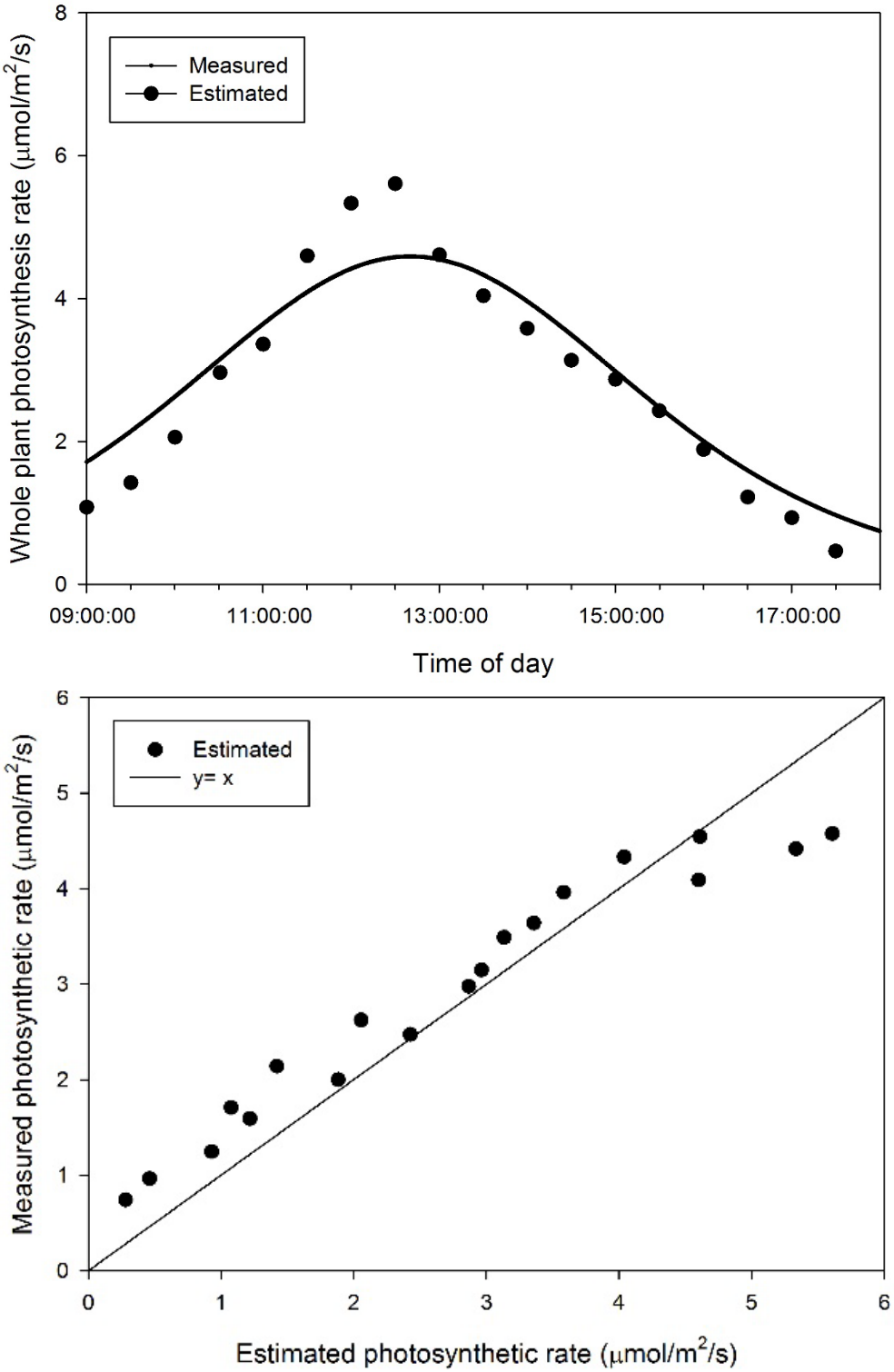

Fig. 5. A validation of measured and estimated photosynthetic rates of the entire plant on 15 Oct. 2014 (R^2 = 0.85).

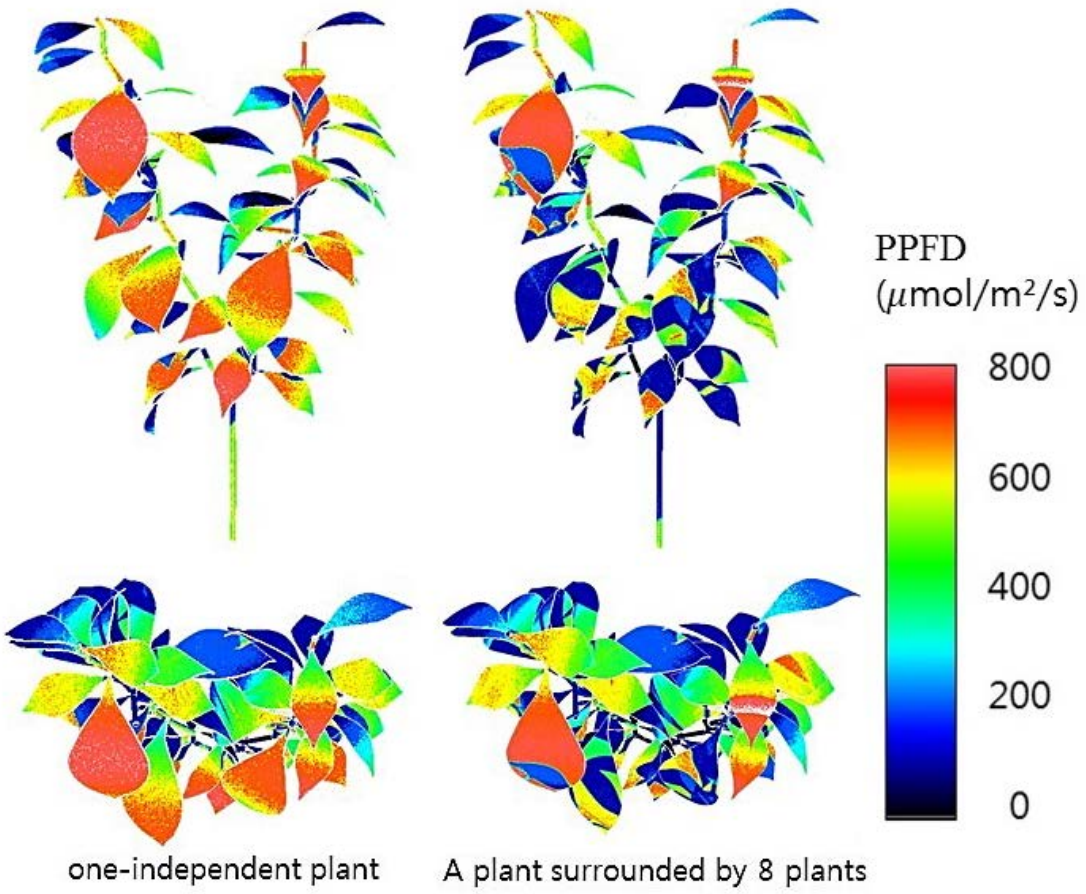

Fig. 6. 3D simulated results of intercepted irradiances of a single plant at 12:00 not surrounded (left) and surrounded (right) by 8 plants.

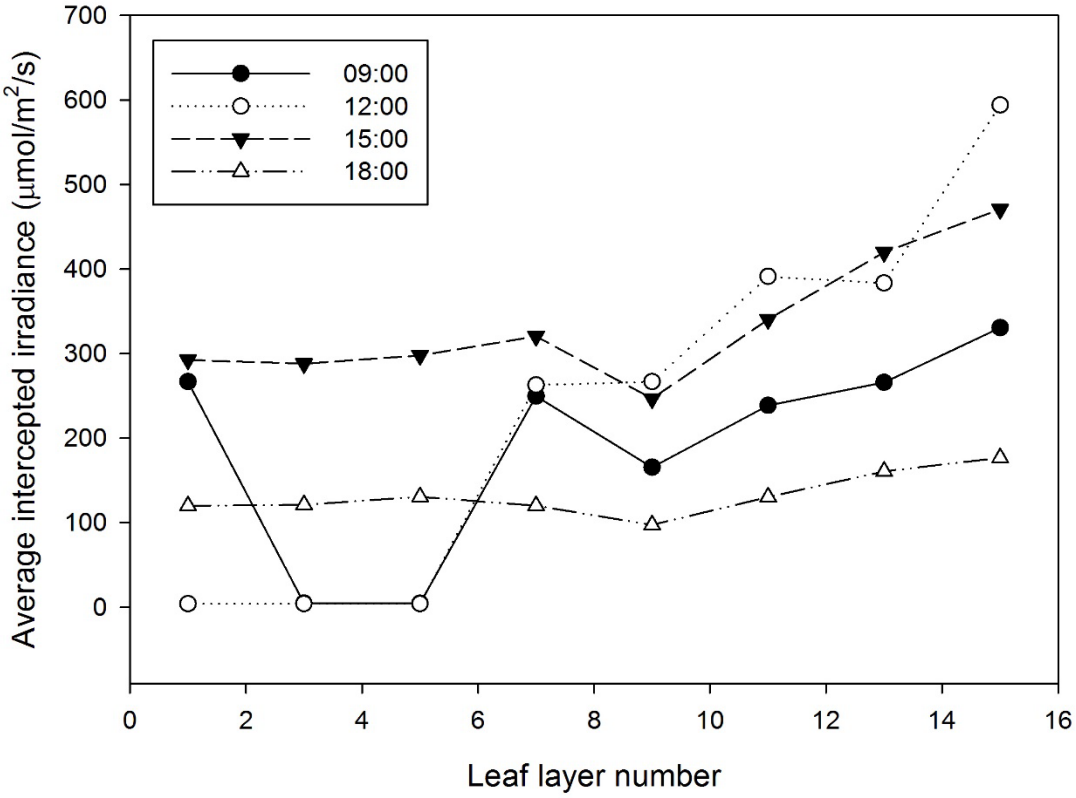

Fig. 7. Estimation of the average intercepted irradiation by leaf layer number from the ray-tracing simulation. The detected sample was a centre plant inside a 5x5 canopy cultivation condition.

LITERATURE CITED

Anten, N.P.R. & During H.J. (2011) Is analyzing the nitrogen use at the plant canopy level a matter of choosing the right optimization criterion?. Oecologia **16**, 293-303.

Boonman, A., Prinsen, E., Gilmer, F., Schurr, U., Peeters, A.J.M., Voesenek, L.A.C.J. & Pons, T.L. (2007) Cytokinin import rate as a signal for photosynthetic acclimation to canopy light gradients. Plant Physiology **143**, 1841-1852.

Caldwell, M.M., Meister, H.-P., Tenhunen, J.D. & Lange, O.L. (1986) Canopy structure, light microclimate and leaf gas exchange of *Quercus coccifera* L. in a Portuguese macchia: measurements in different canopy layers and simulations with a canopy model. Trees **1**, 25-41.

Chen, J.M., Liu, J., Cihlar, J. & Goulden, M.L. (1999) Daily canopy photosynthesis model through temporal and spatial scaling for remote sensing applications. Ecological Modelling **124**, 99-119.

Chen, T.W., Henke, M., de Visser, P.H.B., Sorlin, G.B-., Wiechers, D., Kahlen, K. & Stutzel, H. (2014) What is the most prominent factor limiting photosynthesis in different layers of a greenhouse cucumber canopy?. Annals of Botany **114**, 677-688.

de Pury, D.G.G. & Farquhar, G.D. (1997) Simple scaling of photosynthesis from leaves to canopies without the errors of big-leaf models. Plant, Cell and Environment **20**, 537-557.

der Zande, D.V., Struckens, J., Verstraeten, W.W., Mereu, S., Muys, B. & Coppin, P. (2011) 3D modeling of light interception in heterogeneous forest canopies using ground-based LiDAR data. International Journal of Applied Earth Observation and Geoinformation **13**, 792-800.

Dreccer, M.F., Oijen, M.V., Schapendonk, A.H.C.M., Pot, C.S. & Rabbinge, R. (2000) Dynamics of vertical leaf nitrogen distribution in a vegetative wheat canopy. Impact on canopy photosynthesis. Annals of Botany **86**, 821-831.

Ellsworth, D.S. & Reich, P.B. (1993) Canopy structure and vertical patterns of photosynthesis and related leaf traits in a deciduous forest. Oecologia **96**, 169-178.

Elifis, P., Kratochvilovfi, I., Janous, D., Marek, M. & Masarovicovfi, E. (1989) Stand microclimate and physiological activity of tree leaves in an oak-hornbeam forest I. Stand microclimate. Trees **4**, 227-233.

Escudero, A. & Mediavilla, S. (2003) Decline in photosynthetic nitrogen use efficiency with leaf age and nitrogen resorption as determinants of leaf life span. Journal of Ecology **91**, 880-889.

Evans, J.R. & Poorter, H. (2001) Photosynthetic acclimation of plants to growth irradiance: the relative importance of specific leaf area and nitrogen partitioning in maximizing carbon gain. Plant, Cell and Environment **24**, 755-767.

Field, C. (1983) Allocating leaf nitrogen for the maximization of carbon gain: leaf age as a control on the allocation program. Oecologia **56**, 341-347.

Garcia, R.L., Norman, J.M. & Mcdermitt, D.K. (1990) Measurements of canopy gas exchange using an open chamber system. Remote Sensing Reviews **5**, 141-162.

Gonzalez-Real, M.M. & Baille, A. (2000) Changes in leaf photosynthetic parameters with leaf position and nitrogen content within a rose plant canopy (Rosa hybrid). Plant, Cell and Environment **23**,351-363.

Hikosaka, K. (2005) Leaf canopy as a dynamic system: ecophysiology and optimality in leaf turnover. Annals of Botany **95**, 521-533.

Hikosaka, K. (2014) Optimal nitrogen distribution within a leaf canopy under direct and diffuse light. Plant, Cell and Environment **37**, 2077-2085.

Hirose, T. & Werger, M.J.A. (1987) Maximizing daily canopy photosynthesis with respect to the leaf nitrogen allocation pattern in the canopy. Oecologia **72**, 520-526.

Iio, A., Fukasawa, H., Nose, Y., Kato, S., Kakubari, Y. (2005) Vertical, horizontal and azimuthal variations in leaf photosynthetic characteristics within a Fagus crenata crown in relation to light acclimation. Tree Physiology **25**, 533-544.

Irving, L.J. & Robinson, D. (2006) A dynamic model of Rubisco turnover in cereal leaves. New Phytologist **169**, 493-504.

Johnson, I.R., Thornley, J.H.M., Frantz, J.M. & Bugbee, B. (2010) A model of canopy photosynthesis incorporating protein distribution through the canopy and its acclimation to light, temperature and CO_2. Annals of Botany **106**, 735-749.

Jovicivh, E., Cantliffe, D.J. & Stoffella, P.J. (2004) Fruit yield and quality of greenhouse-grown bell pepper as influenced by density, container, and trellis system. HortTechnology **14**, 507-513.

Kim, H.S., Palmroth, S., Therezien, M., Stenberg, P. & Oren, R. (2010) Analysis of the sensitivity of absorbed light and incident light profile to various canopy architecture and stand conditions. Tree Physiology **31**, 30-47.

Monsi, M. & Saeki, T. (1953) The light factor in plant communities and its significance for dry matter production. Journal of Botany **14**, 22–52.

Norman, J.M. (1980) Interfacing leaf and canopy light interception models in predicting photosynthesis for ecosystem models. CRC Press. **2**, 49-67.

Roux, X.L., Sinoquet, H. & Vandame, M. (1998) Spatial distribution of leaf dry weight per area and leaf nitrogen concentration in relation to local radiation regime within an isolated tree crown. Tree Physiology **19**, 181-188.

Sarlikioti, V., de Visser, P.H.B., Sorlin, G.H.B-. & Marcelis, L.F.M. (2011) How plant architecture affects light absorption and photosynthesis in tomato: towards an ideotype for plant architecture using a functional-structural plant model. Annals of Botany **108**, 1065-1073.

Sharkey, T.D., Bernacchi, C.J., Farquhar, G.D. & Singsaas, E.L. (2007) Fitting photosynthetic carbon dioxide response curves for C_3 leaves. Plant, Cell and Environment **30**, 1035-1040.

Shin, J.W., Ahn, T.I. & Son, J.E. (2011) Quantitative measurement of carbon dioxide consumption of a whole Paprika plant (*Capsicum annumm* L.) using a large sealed chamber. Korean Journal of Horticultural Science and Technology **29**, 211-216.

Schieving, F., Pons, T.L., Werger, M.J.A. & Hirose, T. (1992) The vertical distribution of nitrogen and photosynthetic activity at different plant densities in *Carex acutiformis*. Plant and Soil **14**, 9-17.

Sims, D.A. & Pearcy, R.W. (1992) Response of leaf anatomy and photosynthetic capacity in *Alocasia macrorrhiza* (Araceae) to a transfer from low to high light. American Journal of Botany **79**, 449-455.

Sorlin, G.B-., de Visser, P.H.B., Henke, M., Sarlikioti, V., van der Heijden, G.W.A.M., Marcelis, L.F.M., & Vos, J. (2011) Towards a functional-structural plant model of cut-rose: simulation of light environment, light absorption, photosynthesis and interference with the plant structure. Annals of Botany **108**, 1121-1134.

Stirling, C.M., Aguilera, C., Baker, N.R. & Long, S.P. (1994) Changes in the photosynthetic light response curve during leaf development of field grown maize with implications for modelling canopy photosynthesis. Photosynthesis Research **42**, 217-225.

Tai, N.G., Hung, T.T., Ahn, T.I., Park, J.S. & Son, J.E. (2009) Estimation of leaf area, fresh weight, and dry weight of Paprika (*Capsicum annuum* L.) using leaf length and width in rockwool-based soilless culture. Horticulture Environment and Biotechnology **50**, 422-426.

Thornley, J.H.M. (2002) Instantaneous canopy photosynthesis: analytical expressions for sun and shade leaves based on exponential light decay down the canopy and an acclimated non-rectangular hyperbola for leaf photosynthesis. Annals of Botany **89**, 451-458.

Yin, X. & Struik, P. C. (2009) C_3 and C_4 photosynthesis models: An overview from the perspective of crop modelling. NJAS – Wageningen Journal of Life Sciences **57**, 27-38.

Zhu, X.G., Song, Q. & Ort. D.R. (2012) Elements of a dynamic systems model of canopy photosynthesis. Current Opinion in Plant Biology **15**, 237-244.

ABSTRACT IN KOREAN

군락 내 광합성량은 시설 내 이산화탄소 시비에 대한 전략을 수립하는데 있어 기반 데이터로 이용 능하며 군락의 총 탄소 고정 소모량을 파악함으로써 작물 생육을 예측하는데 매우 중요한

요소이다. 하지만 군락 내 광합성량을 실제 측정하기에는 기술적인 한계가 존재하기 때문에 일반적으로는 수식에 의거한 모델링에 의한 접근이 주로 이루어져 왔다. 여러 모델 중 sunlit-shaded 모델이 가장 강력한 모델로 평가 받고 있는데 이 모델에서는 수광량과 광합성 능력이 캐노피 상단부에서 하단부로 갈수록 지수 함수의 형태로 감소하는 경향을 가진다고 가정하여 군락 광합성 계산을 용이하게 하고 있다. 하지만 실제 상황에서 군락의 수광량은 지역적 위치, 미기후 변수들, LAI, 군락 구조 등 여러 가지 환경변수에 의해 다양한 변화를 보인다. 본 연구의 목표는 삼차원 광선 추적법을 사용하여 파프리카의 군락의 즉각적인 수광량을 정확하게 분석하고 나아가 광합성을 예측하는 것이다. 특정 생육단계를 대표할 수 있는 파프리카 식물을 선정하여 부위별 구조를 실제 측정하고 그래픽 소프트웨어를 이용하여 3D 가상 식물 구조를 디자인하였다. 그리고 실제 구조를 잘 반영한 3D 파프리카를 이용하여 3 차원 광선 추적법을 이용한 시뮬레이션 소프트웨어를 시용해 각 조건에서의 수광량의 수직 분포를 분석하였다. 파프리카는 절간의 개수에 따라 8 개의 층으로 나누고 각 층별에 대한 해석이 이루어졌다. 수광량의 수직적인 분포는 지수 함수의 형태로 감소하는 단일 패턴을 보이지 않고 태양광의 위치와 성질 그리고 시간에 따라서 유동적으로 변화하였으며 특히, 직달광이 하단부에 조사되는 광량, 그리고 산란율에 따라 크게 변화하였다. 또한, 위치 별 광합성 능력을 평가하기 위하여 5 개의 작물을 선정하여 각 층별로 light curve 와 A/C_i curve 를 측정하였다. 이들을 통해 광합성 모델 식에 사용하는 광합성 수용능력에 대한 변수들 V_l, J_m 을 각 위치 별로 구하였고 FvCB 모델의 방정식을 통해 광합성량 추측에 이용되었다. 광합성능력의 경우 역시 모델에서 가정했던 단일 패턴을 띄기 보다 직선적인 수직분포를 보이며 감소하는 것을 확인 할 수 있었다. 각 위치별 수광량 시뮬레이션 데이터와 광합성 능력 변수들을 이용하여 각 위치별 광합성량을 계산하고 이를 합하여 개체 광합성량을 예측하였다. 또한 작물 개체 광합성량을 정확하게 측정하기 위하여 대형 밀폐 챔버를 제작하였다. 3 차원 시뮬레이션에 의하여 예측된 개체 광합성량은 실측 광합성량과 일치하는 결과를 보였다. 이러한 접근 방법을 온실의 실제 군락 조건으로 확장하였을 경우, 이웃 작물에 의한 가림 현상을 반영하면서 작물 위치에 따른 수광량을 추정할 수 있었다.

주요어: 3 차원 모델, 광선 추적법 시뮬레이션, 군락 광합성, 작물 수광량, 광합성 능력, 파프리카, 광합성 모델

학번: 2013-21105